Density Functional Theory Calculations and Vibrational Circular Dichroism of Aromatic Foldamers

Laurent Ducasse,*,† Frédéric Castet,† Alain Fritsch,† Ivan Huc,‡ and Thierry Buffeteau†

Institut des Sciences Moléculaires, UMR CNRS 5255, Université Bordeaux I, 351 Cours de la Libération, 33405 Talence, France, and Institut Européen de Chimie et Biologie, CNRS UMR 5248, Université Bordeaux 1, 2 Rue Robert Escarpit, 33607 Pessac, France

Received: February 28, 2007; In Final Form: April 4, 2007

Ab initio calculations together with vibrational circular dichroism (VCD) have been used for studying the conformations of a quinoline-derived oligoamide bearing a terminal chiral residue. Three helically folded conformers of the dimer, trimer, and tetramer forms of the oligomer were optimized at the density functional theory (DFT) level using the B3LYP functional and the 6-31G* basis set. For each form, the three conformers differ in their helical handedness and in the conformation of the chiral end group. The calculated structures of the tetramer and also the proportions predicted between them based on their calculated Gibbs free energies differences match remarkably well with experimental data collected on an octamer. Specifically, a R-phenethyl terminal group gives rise to a 91:9 ratio between left handed and right handed helices. The predicted VCD spectrum calculated from the Boltzmann population of the individual conformer reproduces very well the experimental VCD spectrum of the tetramer in $CDCl_3$ solution. The DFT calculations performed for the trimer also allow one to assess the preferred handedness of the helix and the conformation of the chiral end group, but the calculated relative populations differ slightly from experimental data. Finally, this study shows that the dimer fragment is not sufficient to obtain valuable information on the conformation of this aromatic oligoamide foldamer.

1. Introduction

In the past 10 years, intense activity has been devoted to the design of new synthetic foldamers, driven mainly by the objective of mimicking some of the functions displayed by peptides and proteins. Various possibilities exist for obtaining helical structures, from the synthesis of rigid molecules in which the helical conformation naturally arises from the minimization of steric strains, to relatively flexible molecules in which the helical conformation is stabilized by multiple noncovalent bonds. Within this framework, multiple helical polymers and oligomers possessing various functions have been prepared and their number still increases due to the development of new synthetic routes.[1] This increase of the variety of helical structures goes hand in hand with the need for efficient and easy to use characterization tools.

The determination of the structural features of new folded structures is usually carried out using a complementary set of experimental techniques, including NMR,[2] circular dichroism in the UV−vis range (CD),[3] and, for rigid oligomer backbones, X-ray crystallography.[1d,4,5] Although less commonly used to assess the conformation of large molecules, vibrational circular dichroism (VCD), which corresponds to the differential absorption of a chiral molecule to left and right handed circularly polarized radiation in the infrared (IR) region, has also proven its usefulness. However, this technique cannot be dissociated from theoretical calculations for a complete analysis of vibrational spectra. It is only the combination of both which provides exploitable information on the absolute configuration and the conformation of the studied molecules.[6] Thus, besides the experimental approaches, the question arises concerning the acceptable compromise to be found between the accuracy of the theoretical model used and the associated computational requirements.

Until now, the properties of helical systems were studied theoretically at different levels of approximations, from molecular mechanics force field (MMFF) calculations, to semiempirical, density functional theory (DFT) and Hartree−Fock (HF) approaches. The conclusion that an approach is better suited than another one depends on the system under consideration, and of course, of the desired physicochemical property. Grimme and Peyrimhoff[7] compared the structures and racemization barriers of helicenes using the semiempirical AM1, HF, and DFT schemes. Their results evidence that HF leads to a poor comparison with experiment, while AM1 performs well and DFT gives the better agreement to experimental data. Blatchly and Tew[8] conclude that MMFF is more appropriate than AM1 or DFT for calculating helical structures and for estimating the relative energies of substituted phenylene ethynylene oligomers. The recent work of Botek et al.[9] on helical pyridine−pyrimidine oligomers also shows the good performance of MMFF calculations, which lead to structures rather close to the X-ray crystallographic ones. On the other hand, semiempirical Hamiltonians and DFT fail to predict the correct geometry of such systems.

Concerning VCD predictions, calculations are usually carried out using DFT methods. Due to their important computational costs, such calculations were in majority restricted to truncated motifs for large systems such as oligopeptides and polynucleotides.[10] Besides, previous ab initio studies of the conformations

* To whom correspondence should be addressed. Fax : (+33) 5 40 00 66 45. E-mail: l.ducasse@ism.u-bordeaux1.fr.
† UMR CNRS 5255.
‡ CNRS UMR 5248.

10.1021/jp071645p CCC: $37.00
Published on Web 05/17/2007

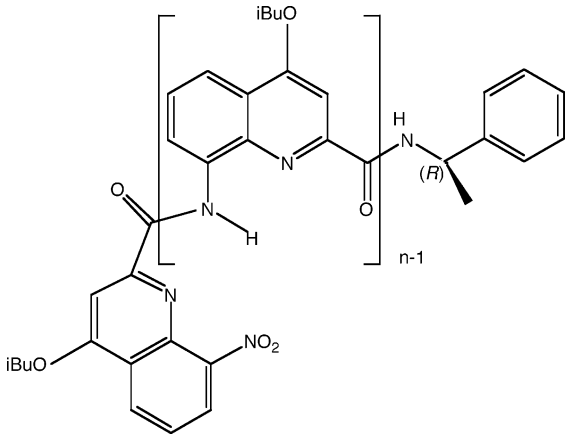

Figure 1. General formula of quinoline-derived chiral oligomers **1**.

of foldamers have been performed on truncated motifs to examine local effects.[11] Thus, they did not involve essential interactions between sites remote in the oligomer sequences that come in proximity upon folding. DFT calculations were also performed on helicenes, which possess a weak conformational freedom,[12] on molecules that possess chiral axes but no chiral centers,[13] and on relatively large objects.[14]

In a recent communication,[15] we tested the prediction that the mixed approach (DFT calculations/VCD experiments) allows one to determine unambiguously the helical handedness of quinoline-derived chiral oligomers **1** reported in Figure 1. The tetramer ($n = 4$) and the octamer ($n = 8$) of **1** have been synthesized both as racemates and as single (*R*) enantiomers.[16,5a,5b] Their helical structure was fully characterized by X-ray crystallography for the two racemates and, in the case of the octamer, for the single (*R*) enantiomer as well. The unit cell of the *R*-octamer contains two conformers, which are involved in a pseudo-centrosymmetry, possessing either right (P) or left (M) handedness. In solution, it has been shown by NMR and CD experiments that the chiral group attached at the end of the oligomer gives rise to chiral helical induction. Moreover, variable conformations at the PhC*−NH linkage can be considered depending on the orientation of the phenyl group with respect to the helical backbone.[5b]

Our recent work clearly demonstrated that DFT calculations together with VCD measurements constitute very accurate tools for elucidating unambiguously the structure of helical molecules, even those containing more than a hundred atoms. However, the huge computational costs required in such studies remain beyond that which is generally considered as a reasonable investment. It is thus crucial to wonder how it would be possible to obtain the essential information, i.e., conformations and helical handedness preferences, at lower cost. Within this framework, one can consider two possibilities: (i) by lowering the level of calculation, which constitutes the most straightforward route but involves the risk of obtaining unreliable results (the level of theory has then to be carefully checked against experimental data and/or more sophisticated levels of calculation); (ii) by decreasing the degree of structural complexity of the system under scrutiny. These two possibilities are considered in this study. The suitability of a semiempirical approach to determine the geometrical structures is first addressed. Then, DFT calculations are performed on simplified molecular structures. Thus, increasingly large oligomers are considered, starting from the dimer to the tetramer, in order to determine the smallest molecular fragment including the essential interactions to assess the handedness as well as the conformation of foldamers **1** and more generally of similar aromatic oligomers.

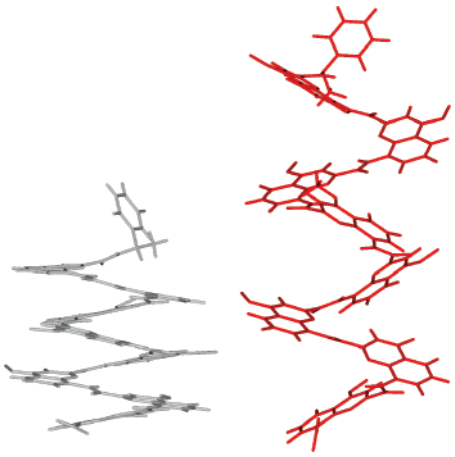

Figure 2. Comparison of the X-ray geometry of the M2 conformation of octamer (left)[5a] to the AM1 result (right).

2. Experimental Measurements and Calculations

VCD Experiments. VCD spectra were recorded with a ThermoNicolet Nexus 670 FTIR spectrometer equipped with a VCD optical bench.[17] In this optical bench, the light beam was focused by a BaF_2 lens (191 mm focal length) to the sample, passing an optical filter (depending on the studied spectral range), a BaF_2 wire grid polarizer (Specac), and a ZnSe photoelastic modulator (Hinds Instruments, Type II/ZS50). The light was then focused by a ZnSe lens (38.1 mm focal length) onto a 1×1 mm^2 HgCdTe (ThermoNicolet, MCTA* E6032) detector. VCD spectra were recorded at a resolution of 4 cm^{-1}, by co-adding 60 000 scans (20 h acquisition time). The sample was held in a variable path length cell with CaF_2 windows. Spectra of tetramer **1** were measured in $CDCl_3$ at a concentration of 0.009 M and at a path length of 250 μm (1 mm in the NH stretching region). Baseline corrections of the VCD spectra were performed by subtracting the raw VCD spectra of the solvent. In all experiments, the photoelastic modulator was adjusted for a maximum efficiency at 1600 cm^{-1} (3000 cm^{-1} for experiments in the NH stretching region). Calculations were done with the standard ThermoNicolet software, using Happ and Genzel apodization, de-Haseth phase-correction, and a zero-filling factor of 1. Calibration spectra were recorded using a birefringent plate (CdSe) and a second BaF_2 wire grid polarizer, following the experimental procedure previously published.[18]

Computational Strategy. The first objective of this work is the determination of the cheapest quantum chemical method for optimizing the geometry of oligomer **1**, the crystal structure being taken as the reference. As already mentioned, semiempirical schemes were shown, in some reported cases, to provide reliable geometries of helical macromolecules while drastically reducing the computational costs compared to ab initio or DFT approaches.[7] Although these methods are known to poorly reproduce the observed vibrational frequencies, their simplicity of implementation constitutes an attractive way to obtain structures at lower cost; such structures can eventually be used as starting guesses in more time-consuming theoretical calculations. Thus, to address the suitability of a semiempirical approach in the present case, the geometry of the octamer was first optimized at the AM1 level starting from the crystal structure.[5a]

Three different conformers, all observed in the solid state, were considered for calculations: one right handed, P2, and two left handed, M2 (in which the terminal phenyl group is aligned with the helical backbone) and M3 (in which the phenyl group points away from the helix). Another conformer M1 (or

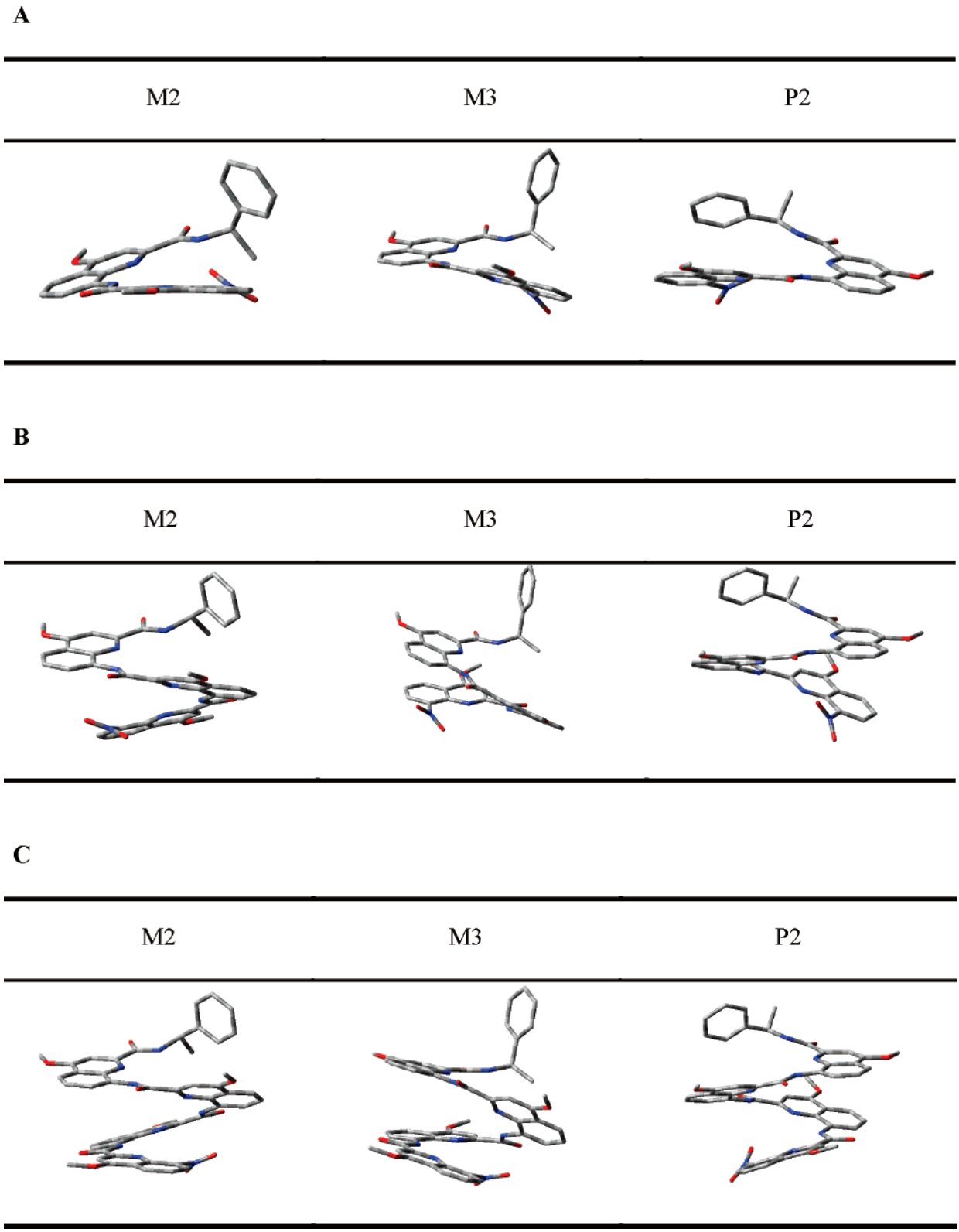

Figure 3. Stick representation of the M2, M3, and P2 conformers in (A) dimeric, (B) trimeric, and (C) tetrameric oligomers.

P1) in which the terminal phenyl group points toward the helix can be considered. The optimized geometry of these conformers has not been calculated due to the stetric hindrance of the end group. Moreover, conformers such as M1 (or P1) were not observed in the solid state, and it seems reasonable to assume that these conformers are not significant in solution.[5b] As shown in Figure 2 for M2, the AM1 optimization gives rise to a much more extended structure than the experimental one. The calculated length of the helix, measured from the N atom bonded to the asymmetric carbon C* to the N atom of the opposite quinoline ring, is equal to 21.6 Å, which corresponds to more than twice the value measured from experimental X-ray data of 10.6 Å. A similar overestimation of the helix extension was previously observed in the case of pyridine−pyrimidine oligomers,[8] as well as in the case of phenylene−ethynylene systems,[9] in which AM1 leads to an overestimation of the helical length

TABLE 1: Structural Parameters of the Optimized Structures of M2, P2, and M3 Conformers of Oligomers 1[a]

oligomer	d [b] (Å)	d_{av} [c] (Å)	L [d] (Å)	L_{av} [e] (Å)
dimer M2	4.47		4.09	
dimer M3	4.41	4.4	4.24	4.2
dimer P2	4.34		4.23	
trimer M2	4.75		5.61	
trimer M3	4.21	4.4	6.02	6.0
trimer P2	4.25		6.28	
tetramer M2 (calc)	4.31		7.71	
tetramer M3 (calc)	4.27	4.3	7.69	7.8
tetramer P2 (calc)	4.28		8.16	
tetramer M2 (expt)[f]	4.15		7.72	
tetramer M3 (expt)[g]	4.06	4.1	7.22	7.5
tetramer P2 (expt)[f]	4.06		7.66	

[a] For tetramer, the experimental data in the solid state are given either from the octamer or from the tetramer. [b] Average quinoline N−N distances between consecutive units. [c] Average of d over M2, M3, and P2. [d] Distance between the first N atom and the last one. [e] Average of L over M2, M3, and P2. [f] From the four terminal units of the crystal structure of an octameric analogue of **1**.[5a] [g] From the crystal structure of the tetramer **1**.[5b]

by about 50 and 20%, respectively. Such a symptomatic behavior disqualifies the semiempirical levels of theory for our study, leaving DFT calculations as the only alternative to provide reliable results.

Regarding the huge computational time necessary to fully optimize the helix geometry within DFT, and further to determine the VCD frequencies and rotational strengths, it is crucial to wonder about the ways to simplify the system prior to calculations. To this end, isobutoxy groups were first removed and replaced by simpler methoxy groups. Moreover, to circumvent the structural complexity of such systems, a systematic study was also performed to determine the smallest molecular fragment which is needed to reproduce the main features of the experimental VCD spectra. This study should be useful in establishing the minimal requirements to obtain the essential information allowing the structure elucidation of foldamers **1**.

The geometry, vibrational frequencies, and VCD intensities of oligomers of increasing size were then calculated at the B3LYP/6-31G(d) level using the Gaussian03 package,[19] which utilizes the magnetic field perturbation method with gauge-invariant atomic orbitals.[20] The octamer being out of reach of our computational resources, the dimer, trimer and tetramer in the three possible conformations P2, M2, and M3 were successively considered. To minimize computational times, a progressive procedure was adopted in geometry optimizations, in which the input geometry of a given conformer was built from the optimized geometry of its analogue of lower size, the smallest dimer structure being optimized beforehand with the help of X-ray information. The largest structures considered in this study ($C_{52}H_{41}O_{10}N_9$) contain 112 atoms and required about 17 days on a monoprocessor IBM P690 computer, while their VCD spectra was obtained in 41 days. To facilitate the comparison with the experimental VCD spectrum, the calculated frequencies were scaled by 0.968 (0.94) and the calculated intensities were converted to Lorentzian bands with half-width of 7 (15) cm^{-1} in the 1150−1800 (3100−3500) cm^{-1} spectral range.

3. Results and Discussion

Structural Parameters. The optimized geometries are gathered in Figure 3, while the relevant structural parameters are reported in Table 1. The average quinoline N−N distance between consecutive units, d_{av}, is quite similar in the different fragments. A value of 4.4 Å is found in the dimer and the trimer, and 4.3 Å in the tetramer. In the latter case, the calculated d_{av} is a little bit larger than the experimental value (4.1 Å). When considering L_{av}, it may be noticed that the difference between the trimer and the dimer is equal to the one between the tetramer and the trimer. The main structural parameters of the largest helix can thus be deduced from those of the smallest fragment. Even if crystal structures are not always representative of ground-state conformations, the optimized structures were found to closely match the helically folded conformations observed in crystals. Specifically, the helical pitch (3.5 Å) and the position of the first carbon of each side chain in the plane of quinoline rings, as well as the number of units per turn (2.5) are very well reproduced by the calculations. This remarkable similarity between the DFT geometries and the X-ray data is illustrated in Figure 4 for the tetramer in its three conformations. Small differences are found in the exact position of the phenyl ring, which, unlike in crystals, does not lie flat on the helix in the optimized P2 and M2 conformers. In the solid state, intermolecular interactions between M2 and P2 conformers within the unit cell constrain the position of the phenyl ring, while, in the optimized structure, an attractive electrostatic interaction between a hydrogen of the phenyl and an amide carbonyl below in the helix is responsible for the phenyl orientation. Moreover, in P2 and M2 conformers, another discrepancy between optimized and crystal structures is observed at the N-termini because of the presence of a nitro group in the optimized structures that forces the first quinoline ring to slightly tilt out of the plane. This nitro group is absent in the crystal structures of P2 and M2 conformers[21] and is present in the crystal structure of the M3 conformer, for which the agreement with the optimized structure is better.

TABLE 2: Gibbs Free Energies, Relative Gibbs Energies, and Populations (at 298 K) of Conformers for the Dimer, Trimer, and Tetramer of Oligomers 1

oligomer	Gibbs energy (hartree)	ΔG (kJ/mol)	population (%)
dimer M2	−1882.873 633	0	91.1
dimer M3	−1882.871 382	5.9	8.1
dimer P2	−1882.869 198	11.6	0.8
trimer M2	−2566.686 602	0	56.0
trimer M3	−2566.685 597	2.6	19.3
trimer P2	−2566.685 851	2.0	24.7
tetramer M2	−3250.503 807	0	83.5
tetramer M3	−3250.501 560	5.9	7.4
tetramer P2	−3250.501 748	5.4	9.1

Population Analysis. The calculated Gibbs free energies of the optimized conformations show that M2 is the most stable conformer whatever the value of n (see Table 2). For even values of n (2 or 4), the left handed helices (M2 and M3) represent more than 90% of the total population, while the right handed helix (P2) represents less than 10%. In particular for $n = 4$, this result matches perfectly the sign and strength of chiral induction of handedness in **1** by the terminal phenethyl−amino group measured in solution by NMR and CD.[5b] The accuracy of theoretical predictions made in the absence of any solvent for a phenomenon observed in solution probably resides in the fact that, for aromatic amide oligomers such as **1**, neither the folded structures nor the strength of helix handedness induction seem to vary much with the solvent (e.g., $CHCl_3$,[5a,b] DMSO,[5a] H_2O,[5c] and MeOH[5c]). For $n = 3$, the contribution of the right handed helix is higher, but the relative population of the left handed helices remains larger than 75%.

VCD Spectra. Our previous communication[15] demonstrated that calculations on tetramers allow one to elucidate unambiguously the structure and the handedness of the major conformer

Figure 4. Side view of the overlaid structures of (left) the optimized structure of the P2 conformation of **1** (red) and the four terminal units of the P2 conformation of an octameric analogue of **1** in the crystal (black);[5a] (middle) the optimized structure of the M2 conformation of **1** (red) and the four terminal units of the M2 conformation of an octameric analogue of **1** in the crystal (black);[5a] and (right) the optimized structure of the M3 conformation of **1** (red), the M3 conformation of **1** in the crystal (black), and the four terminal units of the M3 conformation of an octameric analogue of **1** in the crystal (blue).[5b]

TABLE 3: Frequencies (cm^{-1}), Rotational Strength (10^{-44} esu^2 cm^2), and *m* Value for NH and C═O Vibrations for the Dimer (*n* = 2), Trimer (*n* = 3), and Tetramer (*n* = 4) of the M2, M3, and P2 Conformers[a]

		M2			M3			P2		
	n	freq	RS	*m*	freq	RS	*m*	freq	RS	*m*
NH	2	3531.4	−51.6	2	3528.1	−86.8	2	3517.3	+91.8	2
		3617.3	+63.1	1	3610.8	+73.2	1	3595.5	−28.9	1
	3	3503.6	−52.1	3	3515.5	−107.1	3	3510.9	+103.1	3
		3556.7	−55.8	2	3536.6	−50.8	2	3538.8	+73.1	2
		3601.6	+9.5	1	3585.7	−6.7	1	3582.4	+16.4	1
	4	3520.4	−67.7	4	3514.0	−45.9	4	3521.3	+77.8	4
		3538.3	−67.3	*3* + 2	3532.9	−105.0	*2* + 3	3527.4	+92.3	*2* + 3
		3549.6	−8.9	*2* + 3	3550.0	−21.3	*3* + 2	3549.2	+30.9	*3* + 2
		3605.2	+11.6	1	3583.3	−5.2	1	3589.9	+11.0	1
CO	2	1745.1	−20.8	1	1750.0	−5.3	1	1751.2	+86.2	1
		1750.0	−0.2	2	1755.0	−26.7	2	1756.8	+6.7	2
	3	1744.9	−60.5	3	1740.6	+33.0	1	1741.9	+182.1	1
		1747.0	−5.9	1	1755.5	−102.3	3	1752.5	−46.5	3
		1760.3	−36.8	2	1766.6	−46.6	2	1756.1	+27.4	2
	4	1743.2	−135.8	3	1738.0	+127.6	1	1745.9	+312.8	1
		1749.1	+48.9	1	1750.7	−163.6	3	1749.7	−236.5	3
		1756.8	−203.0	2	1752.2	+28.7	4	1758.0	+167.6	2
		1758.1	+185.4	4	1763.7	−35.1	2	1759.2	−118.7	4

[a] For tetramer, *3* + 2 and *2* + 3 indicate a coupling of two vibrations with a larger weigth on *m*.

in solution. The differentiation between M2 and M3 implies a careful analysis of the VCD spectra, since most vibrators belong to the helical backbone and are not perturbed by the conformation of the terminal chiral moiety. As previously discussed, the amide NH stretching vibrations and the amide I vibration (mainly the C═O stretching vibration) are in fact the only modes significantly affected by the conformation of the terminal chiral group which differentiates the two left handed conformers. This is the reason why we focus in this section on the characteristics of the NH (around 3550 cm^{-1}) and CO stretching vibrations (around 1750 cm^{-1}) as a function of the oligomer size *n*. As mentioned above, the question is to know whether the minimal information allowing one to discriminate the different conformers from the VCD spectra analysis is available from simulations on simpler molecular structures than tetramers. Frequencies and rotational strength (RS) are reported in Table 3 for all NH and CO vibrators of the dimer, trimer, and tetramer in the three conformers. Vibrators are labeled as NH_m (CO_m) with $m = 1$ for the NH (CO) close to C*, $m = 2$ for the nearest neighbor one, and so on, while the last vibrator close to the NO_2 group corresponds to $m = n$. As a whole, whatever the value of *n*, the signs of the rotational strengths in P2 and in M2 (or M3) are opposite; this means that global prediction of handedness from the sign of rotational strength would be valid even for short oligomers. In the following paragraphs, we thus focus our discussion on the comparison of the NH and the CO vibrations in M2 and M3 conformers.

NH Vibration. For each conformer, the higher frequency NH mode corresponds to the vibrator close to C*. This terminal amide connected to the asymmetric carbon derives from an aliphatic amine and thus differs from the other amide groups located in the helical backbone which derive from aromatic amines and are hydrogen bonded to both neighboring quinoline nitrogens. Its vibration is expectedly calculated at a higher wavenumber (≈3600 cm^{-1}). Moreover, when going from the highest frequencies to the lowest ones, the corresponding vibrators appear in the same order: $m = 1$ and 2 for $n = 2$; $m = 1$, 2, 3 for $n = 3$. If one considers that a coupling between $m = 2$ and $m = 3$ occurs in the tetramer, this characteristic is also true for the tetramer: $m = 1$, *2* and *3*, 4. The sign of the RS values involving the NH groups in the helical backbone ($m = 2$, 3, and 4) is negative in each case. Only the terminal amide connected to the asymmetric carbon ($m = 1$) allows to discriminate M2 from M3. The VCD spectra calculated in the NH stretching region for the dimer, trimer, and tetramer of the M2 conformer are reported in Figure 5 and are compared to the experimental spectrum of the tetramer. The VCD spectrum calculated for the tetramer reproduces very well the weak positive band at high frequency and the broad negative contribution at lower frequency, as observed on the experimental spectrum. For the trimer, the absence of coupling between $m = 2$ and 3 implies a splitting of the corresponding VCD bands. Except this splitting, the relative intensities between the VCD bands of $m = 1$ with respect to $m = 2,3$ is well reproduced.

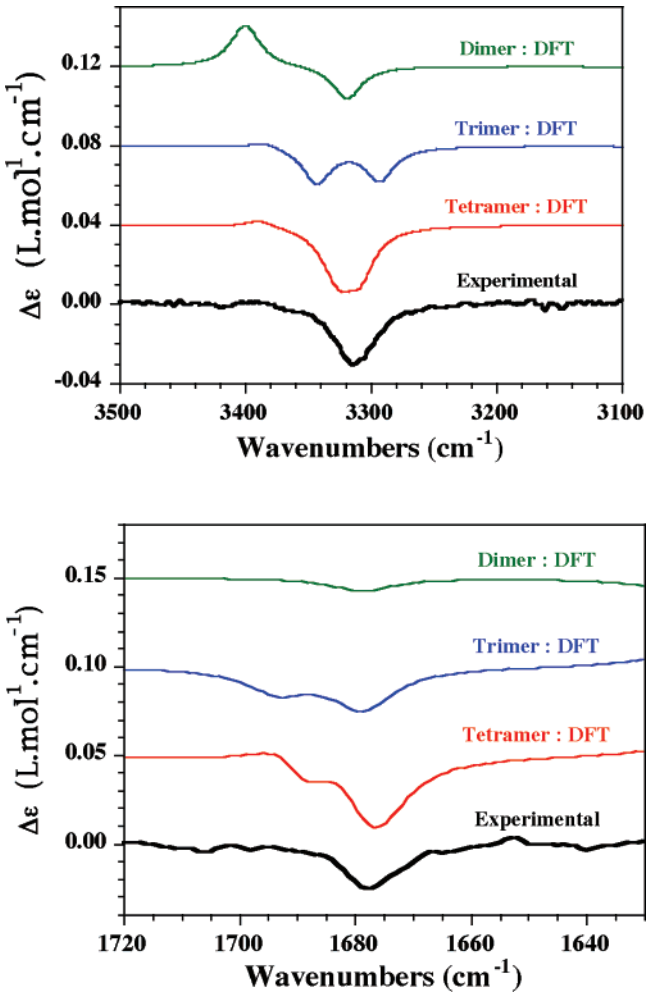

Figure 5. Comparison of the experimental VCD (lower frame, black solid line) spectrum of tetramer **1** with DFT calculated spectra of the M2 dimer (green solid line), trimer (blue solid line), and tetramer (red solid line) conformations of **1**: (Top) NH stretching region; (bottom) C═O stretching region. Calculated DFT spectra are vertically offset for clarity.

Finally, the signs of the VCD bands are correct for the dimer but not their relative intensities.

CO Vibration. It is difficult to extract a tendency from the results reported in Table 3 for the CO vibration. Generally, the carbonyl close to C* is calculated at lower frequency and its associated RS is positive. The negative VCD contribution observed on the experimental spectrum comes from the CO groups in the helical backbone ($m = 2$ and $m = 3$). Consequently, it is necessary to consider the trimer or the tetramer to obtain valuable information on the handedness of the helix.

5. Conclusion

The results presented in this study first demonstrate that DFT calculations associated with VCD experiments provide a detailed and accurate description of the conformation of quinoline-derived oligoamides bearing a terminal chiral residue. Moreover, calculations performed on increasingly large oligomers (e.g., dimer, trimer, and tetramer), allow to determine the smallest fragment including the essential information allowing their unambiguous structure elucidation.

It is found that the calculated structures of the tetramer, as well as the relative populations of the various conformers estimated from Gibbs free energies differences, match remarkably well with experimental data. Moreover, the predicted VCD spectrum nicely agrees with the experimental one, determining the preferential left handed helices of the oligoamide in $CDCl_3$ solution. A more precise examination of the VCD spectrum in the NH stretching region allows in addition to differentiate the conformation of the chiral end group.

DFT calculations performed on the trimer also allow one to assess the handedness of the helix, as well as the conformation of the phenethyl moiety. In this last case, the calculations predict nevertheless a smaller population of (M2 + M3) relative to P2. Finally, this study shows that considering a dimeric oligomer is not sufficient to extract complete structural information. Indeed, although the comparison of the calculated and the experimental VCD spectra allows one to deduce the correct handedness, this molecular fragment is too simple to include valuable information regarding the conformational details in these aromatic oligoamide foldamers.

Acknowledgment. Calculations were carried out on the main frame computers of the M3PEC-Mesocentre of the University Bordeaux I, financed by the "Conseil Régional d'Aquitaine" and the French Ministry of Research and Technology. L.D. and F.C. thank P. Aurel for technical assistance.

Supporting Information Available: Experimental IR and VCD spectra as well as DFT calculated spectra of M2, M3, and P2 tetramers in the NH and CO stretching regions. This material is available free of charge via the Internet at http://pubs.acs.org.

References and Notes

(1) For a review, see: (a) Hill, D. J.; Mio, M. J.; Prince, R. B.; Hughes, T. S.; Moore, J. S. *Chem. Rev.* **2001**, *101*, 3893. (b) Cheng, R. P.; Gellman, S. H.; DeGrado, W. F. *Chem. Rev.* **2001**, *101*, 3219. (c) Schmuck, C. *Angew. Chem., Int. Ed.* **2003**, *42*, 2448. (d) Huc, I. *Eur. J. Org. Chem.* **2004**, 17. (e) Cheng, R. P. *Curr. Opinion Struct. Biol.* **2004**, *14*, 512. (f) Seebach, D.; A. K. Beck, A. K.; Bierbaum, D. J. Chem. Biodiv. **2004**, *1*, 1111. (g) Licini, G.; Prins, L. J.; Scrimin, P. *Eur. J. Org. Chem.* **2005**, 969.

(2) (a) Lee, H.-S.; Syud, F. A.; Wang, X.; Gellman, S. H. *J. Am. Chem. Soc.* **2001**, *123*, 7721. (b) Dolain, C.; Grélard, A.; Laguerre, M.; Jiang, H.; Maurizot, V.; Huc, I. *Chem. Eur. J.* **2005**, 6135.

(3) (a) Glattli, A.; Daura, X.; Seebach, D.; van Gunsteren, W. F. *J. Am. Chem. Soc.* **2002**, *124*, 12972. (b) Sugiura, H.; Nigorikawa, Y.; Saiki, Y.; Nakamura, K.; Yamaguchi, M. *J. Am. Chem. Soc.* **2004**, *126*, 14858. (c) Tanatani, A.; Yokoyama, A.; Azuyama, I.; Takakura, Y.; Mitsui, C.; Shiro, M.; Uchiyama, M.; Muranaka, A.; Kobayashi, N.; Yokozawa, T. *J. Am. Chem. Soc.* **2005**, *127*, 8553.

(4) Appella, D. H.; Christianson, L. A.; Karle, I. L.; Powell, D. R.; Gellman, S. H. *J. Am. Chem. Soc.* **1999**, *121*, 6206.

(5) (a) Jiang, H.; Dolain, C.; Léger, J.-M.; Gornitzka, H.; Huc, I. *J. Am. Chem. Soc.* **2004**, *126*, 1034. (b) Dolain, C.; Jiang, H.; Léger, J.-M.; Guionneau, P.; Huc, I. *J. Am. Chem. Soc.* **2005**, *127*, 12943. (c) Gillies, E.; Dolain, C.; Léger, J.-M.; Huc, I. *J. Org. Chem.* **2006**, *71*, 7931.

(6) (a) Stephens, P. J.; Delvin, F. J. *Chirality* **2000**, *12*, 172. (b) Freedman, T. B.; Cao, X.; Dukor, R. K.; Nafie, L. A. *Chirality* **2003**, *15*, 743, and references therein. (c) Buffeteau, T.; Ducasse, L.; Brizard, A.; Huc, I.; Oda, R. *J. Phys. Chem. A* **2004**, *110*, 4080.

(7) Grimme, S.; Peyrimhoff, S. D. *Chem. Phys.* **1996**, *204*, 411.

(8) Blatchly, R. A.; Tew, G. N. *J. Org. Chem.* **2003**, *68*, 8780.

(9) Botek, E.; Castet, F.; Champagne, B. *Chem. Eur. J.* **2006**, *12*, 827.

(10) (a) Bour, P.; Kubelka, J.; Keiderling, T. A. *Biopolymers* **2002**, *65*, 45. (b) Bodock, L. A.; Fredman, T. B.; Chowdry, B. Z.; Nafie, L. A. *Biopolymers*, **2004**, *73*, 163. (c) Andrushchenko, V.; Wieser, H.; Bour, P. *J. Phys. Chem. B* **2004**, *108*, 389. (d) Bour, P.; Andrushchenko, V.; Kobelac, M.; Maharaj, V.; Wieser, H. *J. Phys. Chem. B* **2005**, *109*, 20579.

(11) (a) Parra, R. D.; Zeng, H.; Zhu, J.; Zheng, C.; Zeng, X. C.; Gong, B. *Chem. Eur. J.* **2001**, *7*, 4352. (b) Parra, R.; Gong, B.; Zeng, X. C. *J. Chem. Phys.* **2001**, *115*, 6036. (c) Doerksen, R. J.; Chen, B.; Liu, D.; Tew, G. N.; DeGrado, W. F.; Klein, M. L. *Chem. Eur. J.* **2004**, *10*, 5008.

(12) (a) Bürgi, T.; Urakawa, A.; Behzadi, B.; Ernst, K. H.; Baiker, A. *New J. Chem.* **2004**, *3*, 332. (b) Botek, E.; Champagne, B.; Turki, M.; André, J. M. *J. Chem. Phys.* **2004**, *120*, 2042.

(13) Freedman, T. B.; Cao, X.; Rajca, A.; Wang, H.; Nafie, L. A. *J. Phys. Chem. A* **2003**, *107*, 7692.

(14) (a) Wang, F.; Zhao, C.: Polavarapu, P. L. *Biopolymers* **2004**, *75*, 85. (b) Urbanova, M.; Setnicka, V.; Delvin, F. J.; Stephens, J. *J. Am. Chem. Soc*. **2005**, *127*, 6700. (c) Brotin, T.; Cavagnat, D.; Dutasta, J. P.; Buffeteau, T. *J. Am. Chem. Soc*. **2006**, *128*, 5533.

(15) Buffeteau, T.; Ducasse, L.; Poniman, L.; Delsuc, N.; Huc, I. *Chem. Commun. (Cambridge)* **2006**, 2714.

(16) Jiang, H.; Léger, J.-M.; Dolain, C.; Guionneau, P.; Huc, I. *Tetrahedron* **2003**, *59*, 8365.

(17) Buffeteau, T.; Lagugné-Labarthet, F.; Sourrisseau, C. *Appl. Spectrosc*. **2005**, *59*, 732.

(18) Nafie, L. A.; Vidrine, D. W. In *Fourier Transform Infrared Spectroscopy*; Ferraro, J. R., Basile, L. J., Eds.; Academic Press: New York, 1982; Vol. 3, p 83.

(19) Frisch, M. J.; Trucks, G. W.; Schlegel, H. B.; Scuseria, G. E.; Robb, M. A.; Cheeseman, J. R.; Montgomery, J. A., Jr.; Vreven, T.; Kudin, K. N.; Burant, J. C.; Millam, J. M.; Iyengar, S. S.; Tomasi, J.; Barone, V.; Mennucci, B.; Cossi, M.; Scalmani, G.; Rega, N.; Petersson, G. A.; Nakatsuji, H.; Hada, M.; Ehara, M.; Toyota, K.; Fukuda, R.; Hasegawa, J.; Ishida, M.; Nakajima, T.; Honda, Y.; Kitao, O.; Nakai, H.; Klene, M.; Li, X.; Knox, J. E.; Hratchian, H. P.; Cross, J. B.; Adamo, C.; Jaramillo, J.; Gomperts, R.; Stratmann, R. E.; Yazyev, O.; Austin, A. J.; Cammi, R.; Pomelli, C.; Ochterski, J. W.; Ayala, P. Y.; Morokuma, K.; Voth, G. A.; Salvador, P.; Dannenberg, J. J.; Zakrzewski, V. G.; Dapprich, S.; Daniels, A. D.; Strain, M. C.; Farkas, O.; Malick, D. K.; Rabuck, A. D.; Raghavachari, K.; Foresman, J. B.; Ortiz, J. V.; Cui, Q.; Baboul, A. G.; Clifford, S.; Cioslowski, J.; Stefanov, B. B.; Liu, G.; Liashenko, A.; Piskorz, P.; Komaromi, I.; Martin, R. L.; Fox, D. J.; Keith, T.; Al-Laham, M. A.; Peng, C. Y.; Nanayakkara, A.; Challacombe, M.; Gill, P. M. W.; Johnson, B.; Chen, W.; Wong, M. W.; Gonzalez, C.; Pople, J. A. *Gaussian03*; Gaussian, Inc.: Pittsburgh, PA, 2003.

(20) Cheeseman, J. R.; Frisch, M. J.; Delvin, F. J.; Stephens, P. J. *Chem. Phys. Lett*. **1996**, *252*, 211.

(21) The crystal data for P2 and M2 conformations of the quinoline tetramer were obtained by truncating the crystal structure of the octamer, hence the absence of a terminal nitro group.